Tetrahedron 66 (2010) 2944–2952

Contents lists available at ScienceDirect

Tetrahedron

journal homepage: www.elsevier.com/locate/tet

Novel quinoxalinophenanthrophenazine-based molecules as sensors for anions: synthesis and binding investigations

Farah S. Raad [a], Ala'a O. El-Ballouli [a], Rasha M. Moustafa [a], Mohammad H. Al-Sayah [b,*], Bilal R. Kaafarani [a,*]

[a] Department of Chemistry, American University of Beirut, Beirut 1107-2020, Lebanon
[b] Department of Biology and Chemistry, American University of Sharjah, Sharjah, United Arab Emirates

ARTICLE INFO

Article history:
Received 5 November 2009
Received in revised form 30 January 2010
Accepted 22 February 2010
Available online 26 February 2010

Keywords:
Quinoxalinophenanthrophenazine
Fluorescent sensors
Anion detection
Chemical sensors
Spectroscopic titrations
NMR titrations

ABSTRACT

The design and synthesis of two novel quinoxalinophenanthrophenazine-based anion sensors are reported. Binding studies of these sensors with an array of mono- and polyatomic anions using UV–vis, fluorescence, and NMR titrations have shown 1:1 and 1:2 sensor-to-anion ratios. Binding constants were calculated for anions, which exhibited high affinity for the sensors, including acetate, benzoate, cyanide, and fluoride ions.

1. Introduction

The design of stable fluorescent chromophores is of great interest due to their application in various fields of research including photoconductors,[1] light emitting diodes,[2] and optical switches.[3] Fluorophores with high quantum yields are perfect candidates for applications in fluorescent sensors due to their innate high sensitivity at low concentration, low cost, and ease of application as a diagnostic tool.[4,5] The design of new anion sensors is a growing field due to the importance of detecting anions for medicinal, industrial, and environmental purposes.[6–11] Among halide ions, for instance, the fluoride ion is vital for prevention of dental caries and treatment of osteoporosis,[12,13] while chloride ion is a tracer of pollution and its detection is essential to monitor intrusion of salt water into drinking water supplies.[14] Similarly, nitrate ion is usually sensed to monitor environmental pollution from agriculture,[14] while the highly toxic cyanide ion, which inhibits cellular respiration and may kill mammals upon binding to a heme group in the active site of cytochrome a_3,[5] is becoming a high-risk environmental contaminant due to industrial release in areas such as gold-mining, electroplating, herbicides, and resins.[5,15] Furthermore, carboxylate and dicarboxylate anions are naturally present in many foods and their consumption (e.g., oxalates) in high levels is hazardous for people with kidney and intestinal disorders.[16]

Compared to cation sensing, anion recognition is more challenging and less explored due to the wide range of geometries and conformations of anions, their significant charge delocalization, and strong hydration.[11,14,17] The design of fluorescent anion sensors relies on various signaling mechanisms such as photo-induced electron transfer (PET),[17,18] intramolecular charge transfer (ICT),[18–20] metal-to-ligand charge transfer (MLCT),[21] and/or excited state intramolecular proton transfer (ESIPT).[22] In a PET sensor, the non-conjugated spacer between the ion receptor and the fluorophore prevents $n\rightarrow\pi$ and $\pi\rightarrow\pi$ ground state interactions between the two components. However, anion binding to the receptor modulates the excited state of the fluorophore causing PET quenching and an increased reduction potential in the receptor.[10,11,23] Nonetheless, receptors that exhibit ICT reveal electronic transitions through a 'push–pull' mechanism accompanied by changes in the dipole moment of the fluorophore, depending on the electron donor/acceptor strengths.[19,20] The binding of the electron-rich anion to ICT receptor alters the electronics of the system leading to either emission enhancement or quenching based on the electronics of binding site. Finally, an ESIPT sensor allows proton transfer from a H-bond donor, in the excited-state, to a H-bond acceptor resulting in two excited species and two emission bands; wherein the red-shifted band arises from an excited tautomer state.[22] In some cases, more than one signaling mechanism is recorded. For example, Gunnlaugsson et al. reported a thiourea PET receptor, which

* Corresponding authors. Tel.: +961 3 151451; fax: +961 1 365217; e-mail addresses: malsayah@aus.edu (M.H. Al-Sayah), bilal.kaafarani@aub.edu.lb (B.R. Kaafarani).

0040-4020/$ – see front matter © 2010 Elsevier Ltd. All rights reserved.
doi:10.1016/j.tet.2010.02.075

exhibited ICT due to the presence of a large dipole moment in the naphthalimide fluorophore.[18] Such a 'push–pull' chromophore usually undergoes dramatic color changes upon H-bonding or proton-transfer to anions producing a colorimetric sensing probe.[18,24]

Several fluorescent anion sensors, which range from highly selective to broad-range detectors, have been reported.[15,25] These sensors are neutral receptors with selective anion recognition elements based on H-bonding, which exhibit high binding strength and selectivity.[26,27] In many examples, the binding motif consists of N–H fragments of amides, ureas, thioureas, or pyrroles that can bind to anions in a reversible manner to allow continuous monitoring.[10,11] For instance, dipyrrolylquinoxalines (DPQ) exhibited a relatively large binding constant toward fluoride ions through a combination of electronic and conformational changes upon H-bonding between the two pyrrole NH groups and the anion.[12,28,29] Further modification of the DPQ systems with electron-withdrawing groups at the pyrrole or quinoxaline subunits led to enhanced anion binding due to the increased acidity of the N–H protons.[30] Another reported example of sensors for cyanide ions was based on dipyrrole carboxamide moiety as a recognition site.[15] The sensor exhibited selective green fluorescence with more than ten-fold enhancement in its emission in the presence of cyanide anions in comparison to the other anions studied. Although many sensors have been reported earlier, there is still a need to develop highly selective and sensitive anion sensors the binding effectiveness of which to the analyte can be monitored easily.

Recently, we have reported a crown-ether-based molecule as a fluorescent sensor for metal ions.[31] The molecule consisted of a tetrasubstituted quinoxalinophenanthrophenazine (TQPP) fluorescent core derivatized with crown ether groups as binding ligands for alkaline and alkali earth metals. In this report, we introduce two new molecules (**1** and **2**) based on the fluorescent core of TQPP but derivatized with sulfonamide groups, which act as binding sites for anions. The function of these molecules as sensors is based on the hydrogen-bonding ability of the N–H bonds of the sulfonamide groups to anions. This binding leads to alteration of the electronic density on the sensor's aromatic system producing significant changes in its absorption and emission profiles. These changes in the photophysical properties of the molecules are associated with the concentration and the type of the introduced anion.

2. Results and discussion

The synthesis of sensors **1** and **2** is illustrated in Scheme 1. The intermediates 2,7-di-*tert*-butyldiketopyrene (**5**) and 2,7-di-*tert*-butyltetraketopyrene (**6**) were prepared by the catalytic oxidation of di-*tert*-butylpyrene (**4**) using ruthenium(III) chloride and sodium

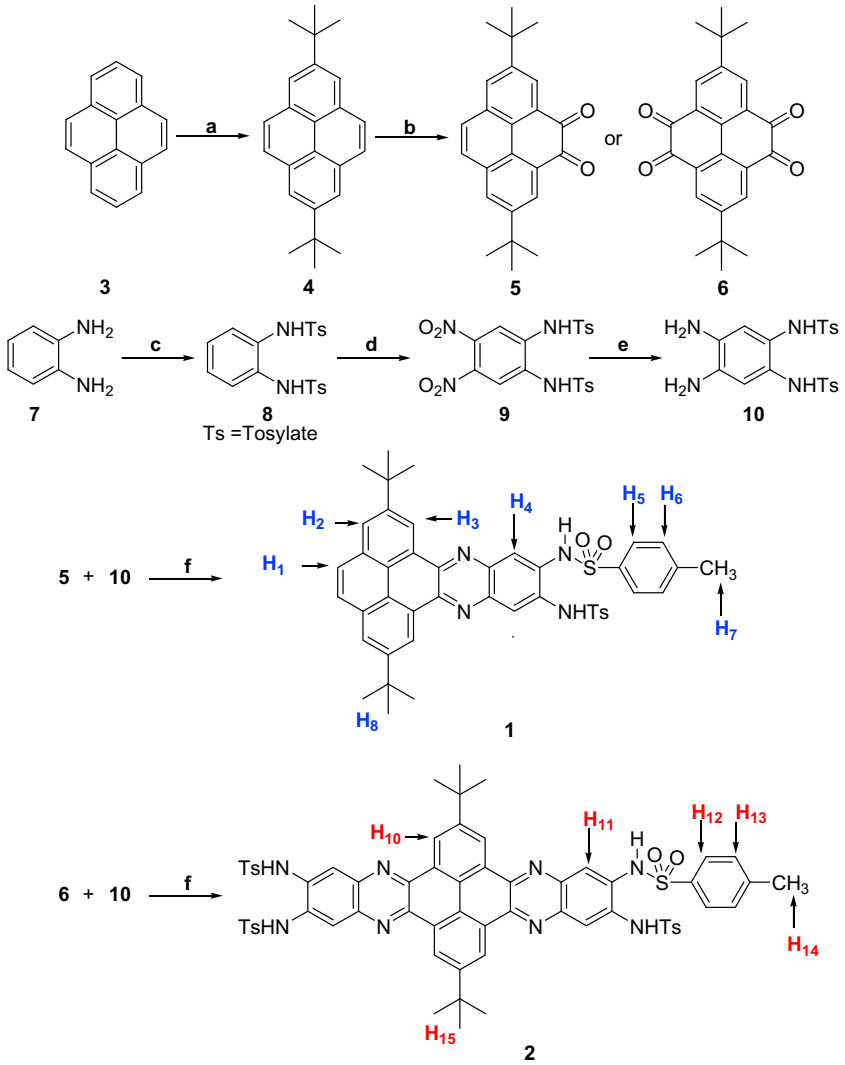

Scheme 1. Synthesis of sensors **1** and **2**. (a) *t*-BuCl, $AlCl_3$; (b) $RuCl_3 \cdot xH_2O$, $NaIO_4$, CH_2Cl_2, MeCN, H_2O; (c) *p*-toluenesulphonyl chloride, pyridine; (d) HNO_3, acetic acid; (e) H_2 (40 psi), Pd/C, ethanol; (f) acetic acid/ethanol.

meta periodate.[32] The reaction of 1,2-phenylenediamine (**7**) with *p*-toluenesulfonyl chloride afforded 1,2-bis(*p*-methylphenylsulfonamido)benzene (**8**),[33] which upon nitration with nitric acid in sulfuric acid produced 1,2-bis(*p*-methylphenylsulfonamido)-4,5-dinitrobenzene (**9**).[34] The reduction of **9** led to 1,2-bis(*p*-methylphenylsulfonamido)-4,5-diaminobenzene (**10**).[35] Condensation of **5** and **10** afforded **1** whereas the condensation of **6** and **10** yielded **2**.

The binding efficacy of sensors **1** and **2** to anions was explored using absorption, emission, and NMR spectroscopies where spectral changes of the sensors were recorded as anion solutions were introduced at increasing concentrations. Typically, the UV–vis spectrum of **1** exhibited characteristic peaks at 280 nm, 355 nm, and 450 nm (Fig. 1). The addition of anions to **1** led to a decrease in the absorbance at 280 nm and to an enhanced absorbance at 355 nm and 450 nm concomitant with a bathochromic shift of peak maximum to 470 nm combined with three isosbestic points at 300 nm, 330 nm, and 430 nm. This behavior indicates strong binding interaction between the sensor and the anion. Figure 1 illustrates the changes observed on the absorption spectra of **1** (5.0 μM in 1:1 CH_2Cl_2/CH_3CN) upon titrating it with a solution of tetrabutylammonium cyanide (TBACN) (1.0 mM in 1:1 CH_2Cl_2/CH_3CN). Similar spectral changes were observed for the interaction of **1** with acetate, benzoate, and fluoride anions while insignificant changes were observed for chloride, bromide, iodide, nitrate, and perchlorate anions.

The change in the absorbance of **1** at 470 nm upon titrating with different anions (Fig. 2) indicated 2–3 times enhancement in the absorbance as one equivalent of the anion was added. When more anion solution was introduced, the change in the absorbance became insignificant. This indicates that sensor had reached a saturation level as it binds to its anion guest through 1:1 binding stoichiometry. This was also suggested by Job's plot (Fig. 1), which indicated maximum absorbance at 0.5 mol fraction. Therefore, the binding isotherms of **1** to acetate, benzoate, cyanide, and fluoride anions were well-fitted to 1:1 binding model with the association constant values presented in Table 1. The binding constants of the other anions were too low to fit the model.

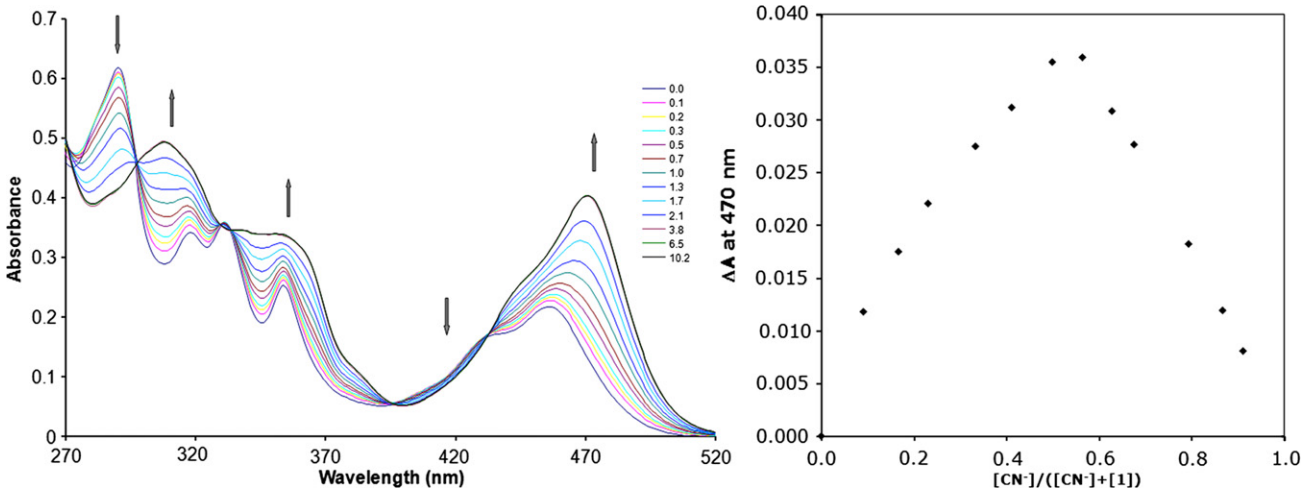

Figure 1. UV–vis spectra (left) of **1** upon titration with solutions of TBACN and Jobs' Plot (right).

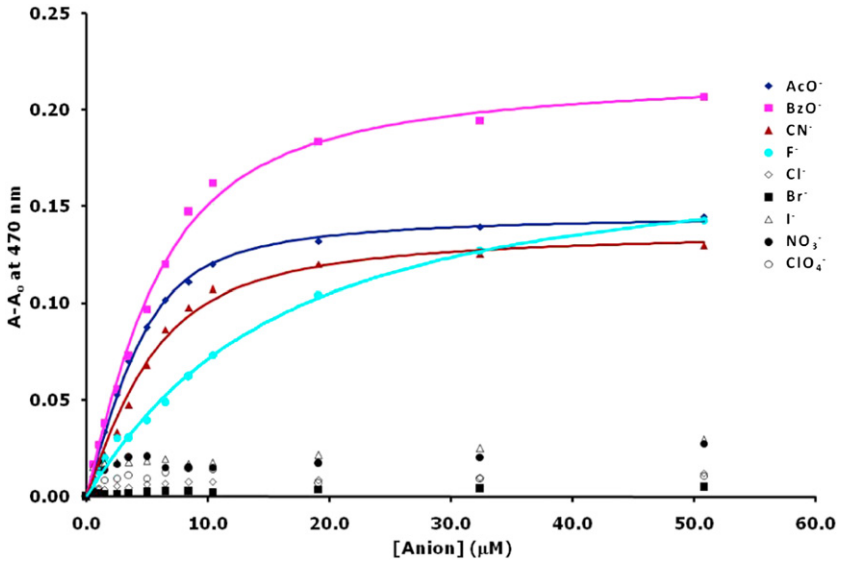

Figure 2. The change in the absorbance of **1** (5.0 μM) at 470 nm upon titration with different anion solutions (1.0 mM) in 1:1 CH_2Cl_2/CH_3CN. The solid lines represent the generated fit-curves from the data sets.

Table 1
Binding constants of sensors **1** and **2** to the corresponding anions[a]

Sensor	**1**	**2**	
Anion	log *K*	log K_1	log K_2
AcO^-	5.2 (5.9)[b]	3.8	4.5
BzO^-	5.3 (5.5)	3.0	4.0
CN^-	6.1 (5.6)	3.5	3.2
F^-	4.4 (4.9)	4.7	4.2

[a] See Supplementary data for more details on K_a calculations.
[b] The values in brackets were calculated from changes in absorbance at 470 nm.

Similar, but more pronounced, changes were observed in the absorption spectrum of **2** (5.0 μM in 1:1 CH_2Cl_2/CH_3CN) upon titrating with TBA solutions (2.0 mM) of acetate, benzoate, cyanide, or fluoride anions. Sensor **2** (Fig. 3) exhibited characteristic peaks at 284 nm, 340 nm, 408 nm, and 433 nm in CH_2Cl_2/CH_3CN (1:1). The addition of fluoride anion resulted in decrease in the absorption of **2** at 284 nm, 408 nm, and 433 nm with enhancements of the peaks at 303 nm, 340 nm, and 470 nm implying very strong binding of the anion to the sensor. Besides, several isosbestic points appeared on the spectra at 294 nm, 382 nm, and 440 nm indicating a clean transfer from the free sensor state to the bound form with the anion. Similar behavior was observed upon titrating with solutions of acetate, benzoate, and cyanide anions.

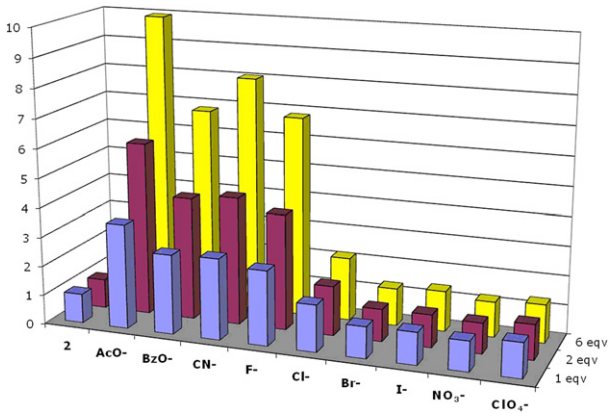

Figure 4. Relative change in the absorbance of **2** (5.0 μM) at 470 nm upon introduction of different anion solutions in 1:1 CH_2Cl_2/CH_3CN.

The relative change in the absorbance of **2** at 470 nm upon titrating with different anions (Fig. 4) indicated 6–10 times enhancement in the absorbance at 470 nm upon the addition of more than two equivalents of the anion. Absorbance increased as the anions were added until about three equivalents of the anion had been added but as more anion solution was introduced, the change in the absorbance became insignificant. This indicated that the sensor binding had reached a saturation level of **2** as it binds to its anion guest through 1:2 binding stoichiometry. Job's plot (Fig. 3) supported this conclusion as it indicates maximum absorbance at a mole fraction of 0.67 of the anion. Such behavior was specifically noticed with acetate, benzoate, cyanide, and fluoride anions while other anions showed insignificant effect on the absorbance of **2**.

The binding of anions to **1** and **2** resulted in dramatic changes in emission spectra of each sensor. Sensor **1** exhibited an emission maximum at 500 nm upon excitation at 350 nm in CH_2Cl_2/CH_3CN (1:1) solution. However, titrating sensor **1** with acetate, benzoate, cyanide, or fluoride anions led to enhancement of the sensor's emission with a bathochromic shift of the peak to 550 nm. This is an indication of the stabilization of the charged-transfer emission state of the sensor by the anion. Figure 5 shows the changes in the emission of **1** upon titrating with acetate and cyanide anions. The other anions (chloride, bromide, iodide, nitrate, and perchlorate) had little effect on the emission of **1**.

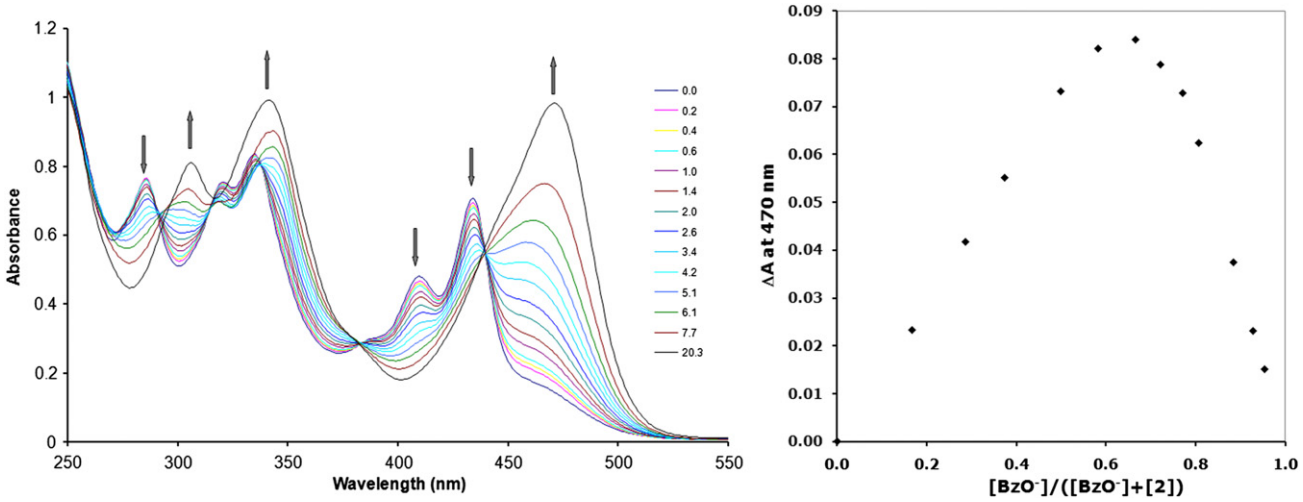

Figure 3. UV–vis spectra (left) for **2** upon titration with solutions of TBAF and Job's plot (right).

The relative change in the emission of **1** at 550 nm is shown as a function of the mole ratio of the sensor to the anion in Figure 6. The emission of **1** at 550 nm increased quickly as anion solution was titrated in until it reached a constant value after one equivalent of the anion (acetate, benzoate, and cyanide) had been added. The fluoride anion required the addition of more than three equivalences of anion until it reached constant emission intensity. Besides, it was noticed that the highest response was for cyanide anion with about three times enhancement in emission followed by acetate, benzoate, and fluoride anions, respectively. This may be attributed to the higher charge density and basicity of the cyanide anion as compared to that of stabilized carboxylate and fluoride anions.[10]

The emission spectrum of **2** was significantly different from that of **1** due to the symmetrical structure of the chromophore. In the absence of anions, sensor **2** exhibited emission maximum at 450 nm with a shoulder emission at 470 nm (Fig. 7) upon excitation at 350 nm. As anion (acetate, benzoate, cyanide, or fluoride) solution was titrated in, the emission at 450 nm decreased until it reached its minimum after one equivalent of the anion had been

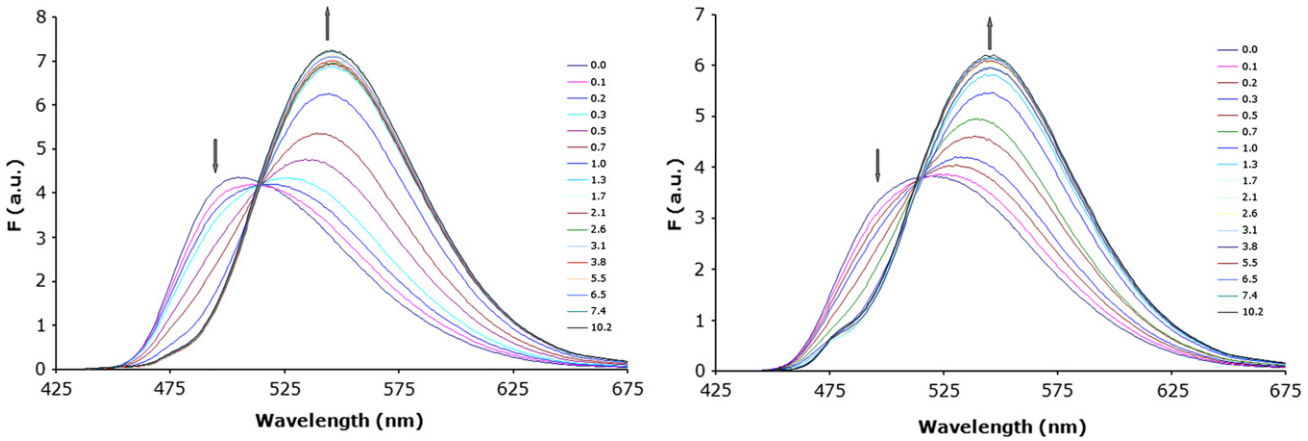

Figure 5. Emission spectra of **1** (5.0 μM) upon addition of TBAOAc (left) and TBACN (right) solutions (1.0 mM) in 1:1 CH_2Cl_2/CH_3CN.

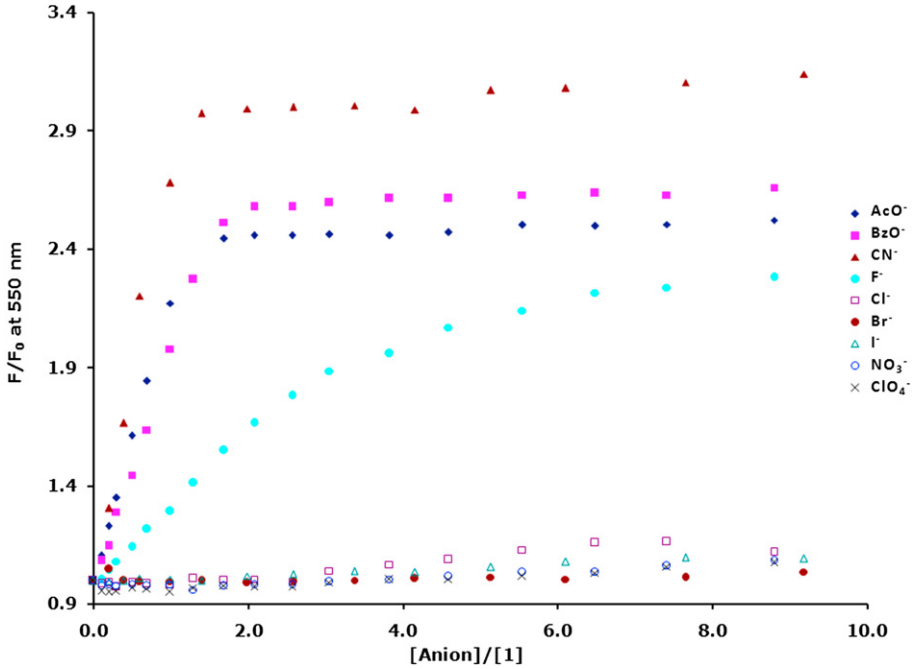

Figure 6. Relative change in the emission of **1** (5.0 μM) at 550 nm upon titration with different anion solutions (1.0 mM) in 1:1 CH_2Cl_2/CH_3CN.

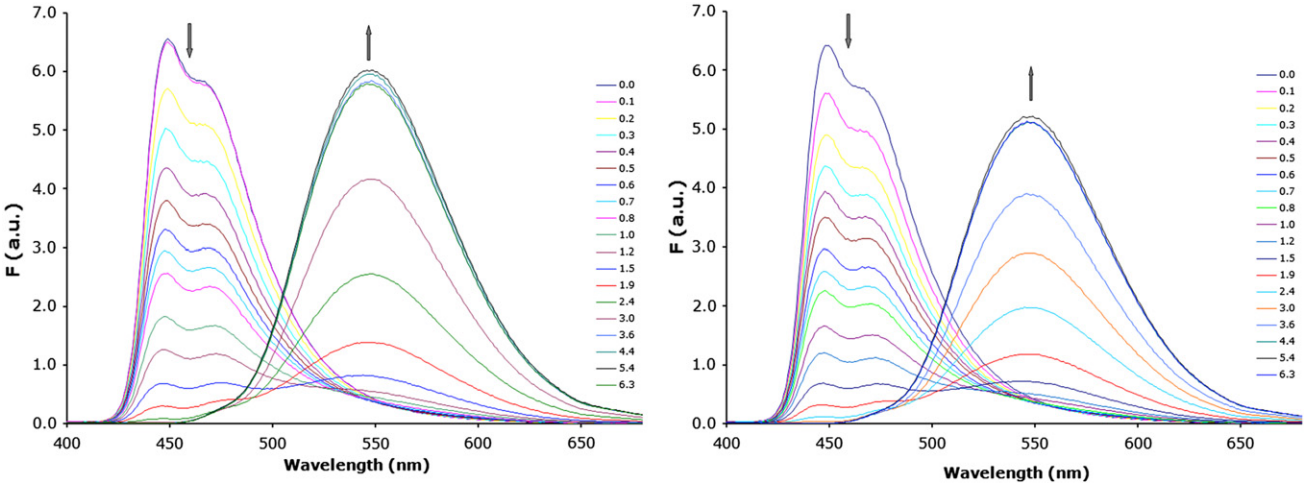

Figure 7. Emission spectra of **2** (5.0 μM) upon addition of TBAF (left) and TBAOAc (right) solutions (2.0 mM) in 1:1 CH_2Cl_2/CH_3CN.

added, Figure 8. As the anion amount increased above two equivalents of **2**, a new emission peak started to appear at 550 nm, Figure 7. This peak continued to increase until it reached its maximum at four equivalents of the anion, Figure 8. Comparing the effect of each anion on the emission at 450 nm and 550 nm clearly indicates that sensor **2** had higher affinity for acetate, benzoate, cyanide, and fluoride anions (vide infra).

signals of the aromatic protons are shown as the concentration of the fluoride anion was increased. The signals of H_2, H_4, and H_6 shifted upfield from 8.272 ppm, 7.991 ppm, and 7.247 ppm to 8.173 ppm, 7.956 ppm, 7.109 ppm, respectively. This was attributed to the increase of the electronic density of the aromatic system upon hydrogen bonding between the N–H protons and the anion (through-bond effect). Meanwhile, the signal of H_5 shifted down-

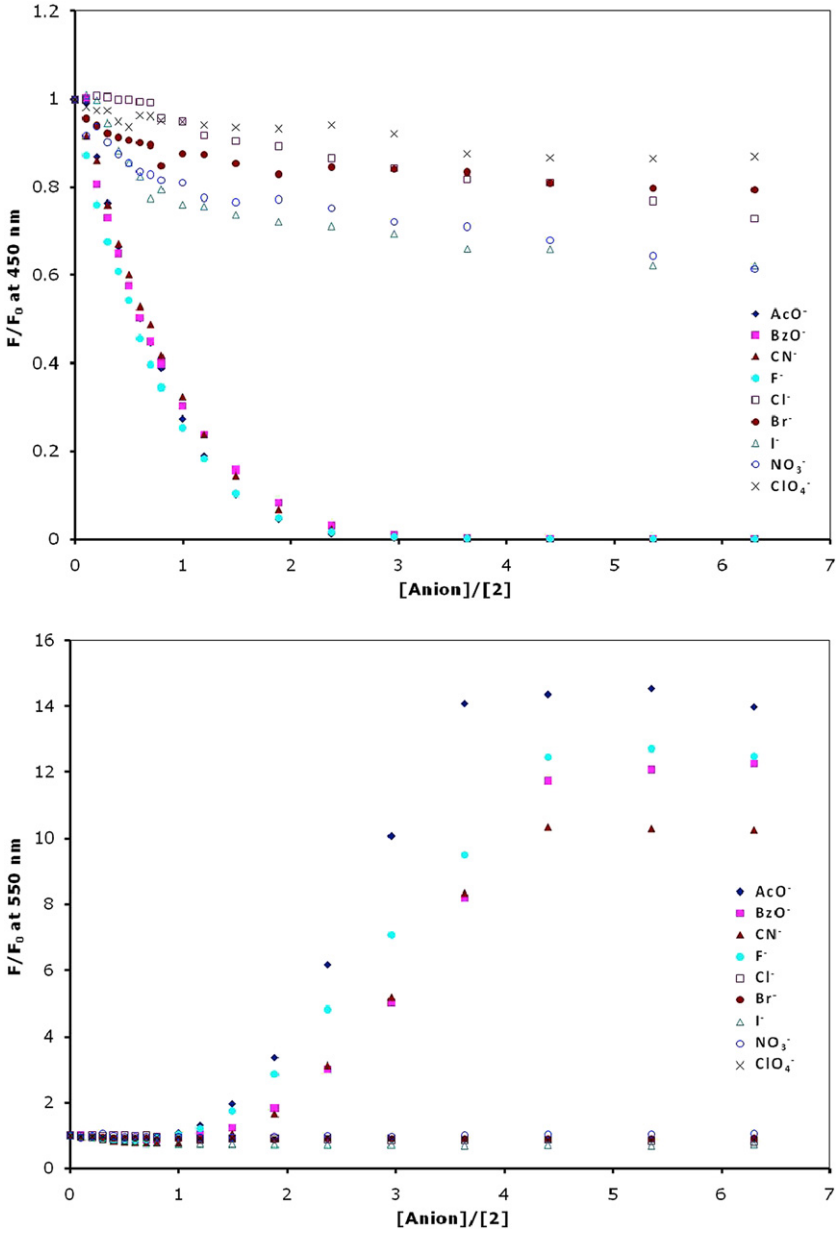

Figure 8. Relative change in the emission of **2** (5.0 μM) at 450 nm (top) and 550 nm (bottom) upon titration with different anion solutions (2.0 mM) in 1:1 CH_2Cl_2/CH_3CN.

NMR titrations of **1** and **2** further supported the trend of anion binding as observed in photophysical studies. The chemical shifts of the N–H protons of the sulfonamide groups, which are associated with the binding process did not appear in the proton NMR spectrum, even before anion was added, probably due to chemical exchange with the solvent. Thus, the chemical shifts of the C—H neighboring protons were monitored as aliquots of anion solution were added into solution of the sensors in $CDCl_3$ (**1**) and DMSO-d_6 (**2**). Figure 9 shows partial proton NMR spectra of **1** where the

field from 7.738 ppm to 7.837 ppm due to through-space effect of the anion bound at close proximity to these protons. With respect to H_3, there was hardly any effect on the chemical shift of the signal corresponding to these protons.

The change in the chemical shift of the neighboring protons to the binding site was also used to calculate the binding constants of the sensor to the anions. The chemical shift of H_4 decreased upon the addition of the anions and it reached a constant value once one equivalent of the anion had been added indicating strong binding

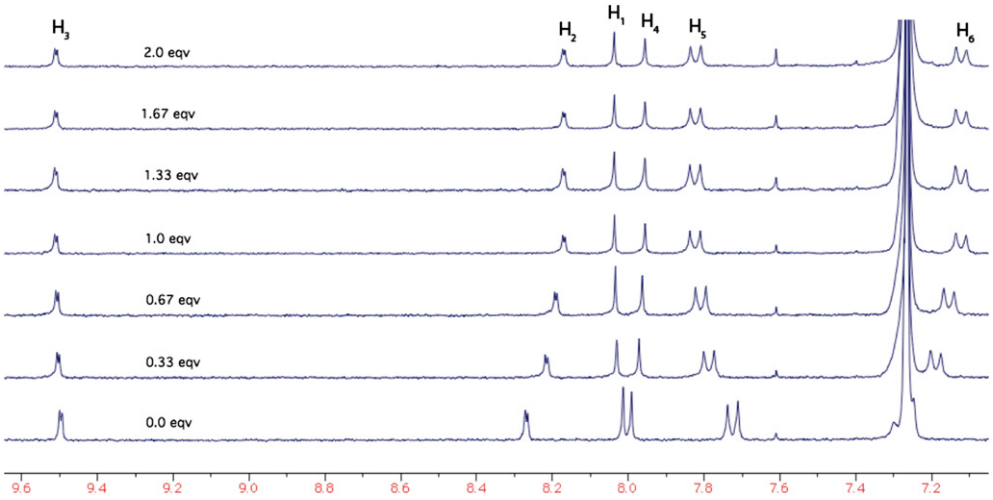

Figure 9. Partial ^{1}H NMR spectra of **1** (1.0 mM) upon titrating with TBAF solution (10 mM) in $CDCl_3$.

with 1:1 stoichiometry. For example, the addition of TBAOAc solution to a solution of **1** in $CDCl_3$, Figure 10, caused to the shift of the signal of H_4 from 7.991 ppm to 7.956 ppm. Job's plot of this titration, based on the change in the chemical shift, indicated 1:1 binding stoichiometry and the isotherm fitted to 1:1 binding model with K_a of 1.75×10^5 M^{-1}. The values of the binding constants calculated through NMR titrations for all anion were in good agreement with the values obtained through absorbance studies, Table 1.

electronic density of the aromatic ring through bond-effect. Meanwhile, the through-space electrostatic effect was insignificant due to the high dielectric constant of DMSO leading to an upfield shift of H_{12} instead of a downfield shift (as was noticed for H_5 of sensor **1**). The shifts of these signals were minimal after the addition of two equivalents of the anion which implied 1:2 binding stoichiometry of **2** to the anion. Besides, the observed broadness in the signals of H_{11} and H_{13} can be attributed to the slow conformational changes that

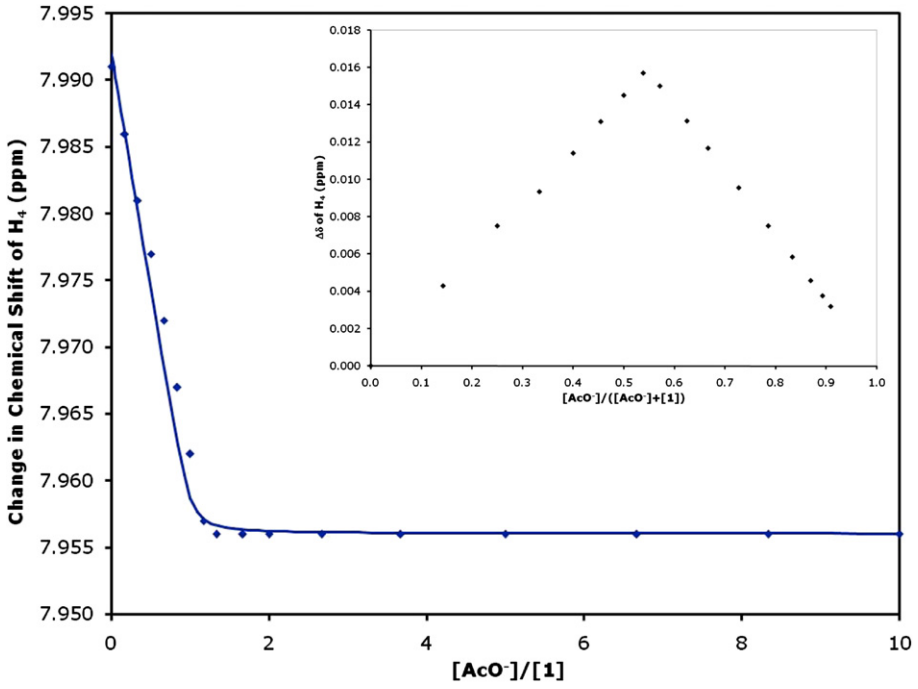

Figure 10. Change in the chemical shift of H_4 of **1** (1.0 mM) upon titrating with TBAOAc solution (10 mM) in $CDCl_3$ and Job's plot (inset) for the binding.

NMR titrations of **2** were conducted in DMSO-d_6 solvent due to the low solubility of **2** in $CDCl_3$ at 1 mM concentration. Figure 11 exhibits partial proton NMR spectra of **2** that include the signals corresponding to the aromatic protons H_{10}, H_{11}, H_{12}, and H_{13}, at increasing concentrations of acetate anion. The signals of H_{11}, H_{12}, and H_{13} shifted upfield from 7.941 ppm, 7.803 ppm, and 7.411 ppm to 7.714 ppm, 7.763 ppm, and 7.286 ppm, respectively, as acetate anions were added. These changes were in accordance with the increase of need to take place around the sulfonamide group to accommodate the anion. The signals regained their sharpness once the sensor was saturated with the anion (>2 equiv). Finally, the binding constants of **2** were calculated (Table 1) by fitting the changes in the chemical shift of H_{11} to a 1:2 binding model using non-linear least square regression methods (see Supplementary data).

On the other hand, the signal of H_{10} exhibited an interesting behavior over the course of the titration, Figure 12. As the anion was

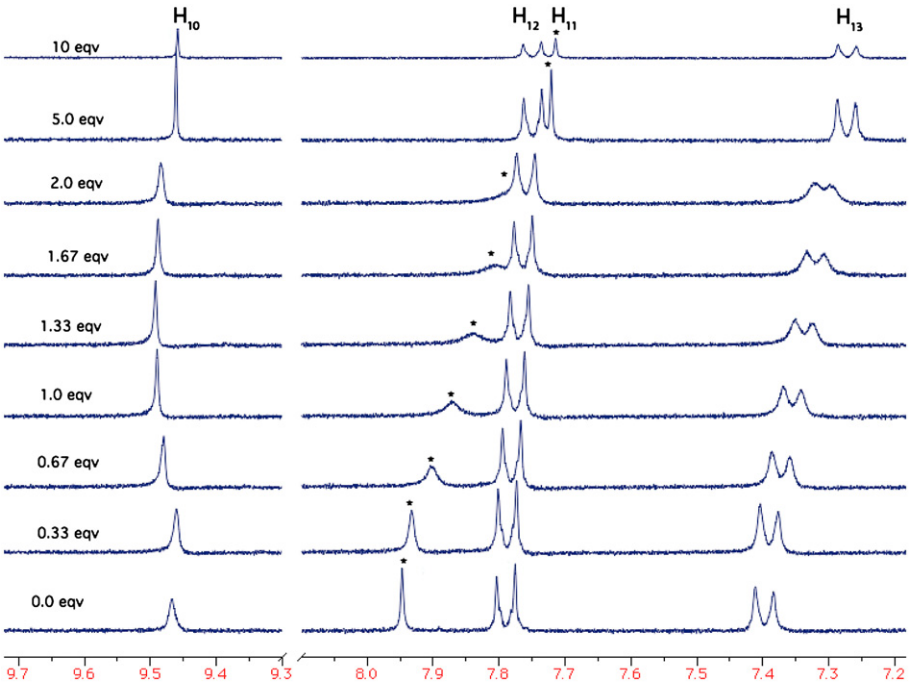

Figure 11. Partial ^{1}H NMR spectra of **2** (1.0 mM) upon titrating with TBAOAc solution (10 mM) in DMSO-d_6.

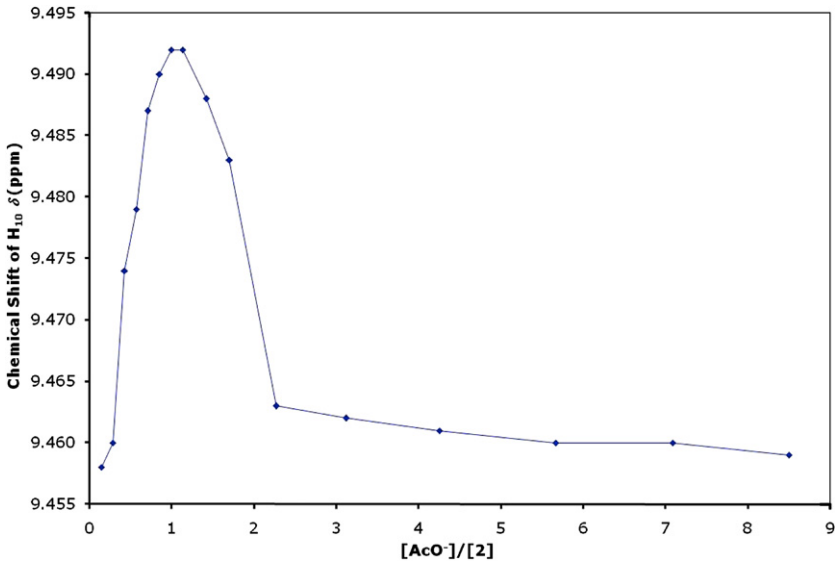

Figure 12. The change in the chemical shift of H_{10} of sensor **2** (1.0 mM) upon titrating it with TBAOAc solution (10 mM) in DMSO-d_6.

added, the signal of H_{10} shifted downfield due to the electrostatic (through-space) effect of the increased electronic density on the neighboring N-atom of the TQPP system. When the added acetate became more than one equivalent, the signal started to shift back upfield where it stopped after two equivalents had been added. This implies that as the second binding site of the sensor became engaged in binding the anion, the increased electronic density through-bond effect overcame the electrostatic effect of the neighboring N-atom of TQPP shifting the signal upfield.

3. Conclusion

In summary, two quinoxalinophenanthrophenazine-based molecules have been synthesized and were shown to be effective fluorescent sensors for several anions. Sensors **1** and **2** have exhibited high affinity to acetate, benzoate, cyanide, and fluoride ions reflected through the changes in the absorption and emission spectra of the sensors upon the addition of the ions at different concentrations. These changes can be attributed to the alterations of the electronic density of the chromophore and, hence the 'push–pull' mechanism upon anion binding. Meanwhile, deprotonation of the sensors by the anions was considered unlikely at such anion-to-sensor ratios. This conclusion is supported by the lack of significant color change or dramatic shifts in absorbance spectra of the sensors upon addition of anions. Also, NMR titrations supported these finding and the mode of binding of these sensors through the sulfonamide groups. For example, if deprotonation was taking place, a triplet signal would have been observed in the NMR spectrum at

16 ppm (corresponding to H_2F^-) upon titrating the sensors with the fluoride anion.[18] Finally, the low acidity of sulfonamide (pK_a=16 in DMSO)[36,37] as compared to acetic acid (pK_a=12 in DMSO) and benzoic acid (pK_a=11 in DMSO) makes deprotonation of the sensors by the acetate or the benzoate anions unfeasible even if 10 M equivalents of the anion were present.

4. Experimental

4.1. General

Chemicals and solvents were purchased from Acros. Standard grade silica gel (60 Å, 32–63 μm) and silica gel plates (200 μm) were purchased from Sorbent Technologies. Reactions that required anhydrous conditions were carried out under argon in oven-dried glassware. A Bruker spectrometer was used to record the NMR spectra. $CDCl_3$ and DMSO-d_6 were the solvents for NMR measurements and chemical shifts relative to TMS at 0.00 ppm are reported in parts per million (ppm) on the δ scale. Elemental analyses were performed at Atlantic Microlab Inc., Norcross, GA.

4.1.1. Sensor ***1****.* 2,7-Di-*tert*-butyldiketopyrene (**5**)[32] (230 mg, 0.67 mmol) and 1,2-bis(*p*-methylphenylsulfonamido)-4,5-diaminobenzene (**10**)[35] (300 mg, 0.67 mmol) were refluxed in a mixture of (1:1) ethanol/acetic acid (60 mL) for 24 h. The reaction mixture was filtered and washed with cold ethanol to yield a fluorescent green solid of **1** (385 mg, 77%), mp >300 °C. ^{1}H NMR (300 MHz, DMSO-d_6): δ 9.40 (2H, d, J=1.8 Hz), 8.46 (2H, d, J=2.1 Hz), 8.16 (2H, s), 7.94 (2H, s), 7.79 (4H, d, J=8.4 Hz), 7.39 (4H, d, J=8.4 Hz), 2.35 (6H, s), 1.60 (18H, s). ^{13}C NMR (75 MHz, $CDCl_3$): δ 149.8, 144.6, 144.3, 140.4, 135.0, 132.2, 131.1, 129.9, 128.5, 127.7, 126.2, 124.3, 124.2, 121.7, 35.52, 21.61. Anal. Calcd for $C_{44}H_{42}N_4O_4S_2$: C, 70.00; H, 5.61; N, 7.42. Found: C, 69.90; H, 5.50; N, 7.30.

4.1.2. Sensor ***2****.* 2,7-Di-*tert*-butyltetraketopyrene (**6**)[32] (150 mg, 0.40 mmol) and 1,2-bis(*p*-methylphenylsulfonamido)-4,5-diaminobenzene (**10**)[35] (360 mg, 0.81 mmol) were refluxed in a mixture of (1:1) ethanol/acetic acid (60 mL) under argon for 24 h. The reaction mixture was filtered and washed with cold ethanol to yield a yellow solid, which was triturated using hot toluene via Soxhlet extraction to yield **2** (330 mg, 70%), mp >300 °C. ^{1}H NMR (300 MHz, DMSO-d_6): δ 9.51 (4H, s), 7.93 (4H, s), 7.78 (4H, d, J=6.9 Hz), 7.38 (4H, d, J=7.2 Hz), 2.35 (12H, s), 1.60 (18H, s). ^{13}C NMR (75 MHz, DMSO-d_6): δ 150.6, 143.9, 141.7, 139.3, 136.6, 133.5, 129.9, 128.7, 126.9, 124.5, 123.5, 118.7, 35.3, 31.4, 20.9. Anal. Calcd for $C_{64}H_{58}N_8O_8S_4$: C, 64.30; H, 4.89; N, 9.37. Found: C, 64.06; H, 4.91; N, 9.12.

4.1.3. Spectroscopic titration. A solution of the sensor (5 μM, 2 mL) in CH_2Cl_2/CH_3CN (1:1) placed into a 1×1 cm cuvette was titrated with a solution of the anion (1.0 mM or 2.0 mM, CH_2Cl_2/CH_3CN (1:1)) that contained the sensor (5 μM). Aliquot amounts of the anion solution were added to the cuvette via a syringe until a total of six or more equivalents of the anion had been added (the number of additions was around 20 with an increase in the amount of anion solution added). The UV–vis spectrum and emission spectrum (λ_{ex}=350 nm) were scanned after each addition.

4.1.4. ^{1}H NMR titration. A solution of the sensor (1 mM, 600 μL) in $CDCl_3$ (**1**) or DMSO-d_6 (**2**) placed in an NMR tube was titrated with a solution of the anion (10 mM). Aliquot amounts of the anion solution were added to the NMR tube via a syringe until a total of ten equivalents of the anion were added (the number of additions was around 17 with an increase in the amount of anion solution added). A ^{1}H NMR spectrum was recorded after each addition and the chemical shifts of the aromatic protons were recorded. The collected data was analyzed using a non-linear least square regression program to fit the data to a theoretical model of a 1:1 for sensor **1** and 1:2 for sensor **2** (see Supplementary data).

Acknowledgements

This work was supported by the University Research Board (URB) of the American University of Beirut, American University of Sharjah (grant # FRG08-01), the Royal Society of Chemistry, and by the Petroleum Research Foundation of the American Chemical Society (grant #: 47343-B10). The authors are grateful for this support.

Supplementary data

Absorption titration spectra of the sensors, calculations of binding constants, and the curve fit of NMR data are provided in the Supplementary data. Supplementary data associated with this article can be found, in the online version, at doi:10.1016/j.tet.2010.02.075.

References and notes

1. Kitamura, N.; Inoue, T.; Tazuke, S. *Chem. Phys. Lett.* **1982**, *89*, 329–332.
2. Tao, Y.; Wang, Q.; Yang, C.; Wang, Q.; Zhang, Z.; Zou, T.; Qin, J.; Ma, D. *Angew. Chem., Int. Ed.* **2008**, *47*, 8104–8107.
3. Cuisdo, J.; Deniz, E.; Raymo, F. M. *Eur. J. Org. Chem.* **2009**, 2031–2045.
4. Aldakov, D.; Palacios, M. A.; Anzenbacher, P., Jr. *Chem. Mater.* **2005**, *17*, 5238–5241.
5. Lee, K.-S.; Kim, H.-J.; Kim, G.-H.; Shin, I.; Hong, J.-I. *Org. Lett.* **2008**, *10*, 49–51.
6. Gale, P. A. *Coord. Chem. Rev.* **2001**, *213*, 79–128.
7. Sessler, J. L.; Davis, J. M. *Acc. Chem. Res.* **2001**, *34*, 989–997.
8. de Silva, A. P.; Gunaratne, H. Q. N.; Gunnlaugsson, T.; Huxley, A. J. M.; McCoy, C. P.; Rademacher, J. T.; Rice, T. E. *Chem. Rev.* **1997**, *97*, 1515–1566.
9. Beer, P. D.; Gale, P. A. *Angew. Chem., Int. Ed.* **2001**, *40*, 486–516.
10. Amendola, V.; Esteban-Gomez, D.; Fabbrizzi, L.; Licchelli, M. *Acc. Chem. Res.* **2006**, *39*, 343–353.
11. Gunnlaugsson, T.; Glynn, M.; Tocci, G. M.; Kruger, P. E.; Pfeffer, F. M. *Coord. Chem. Rev.* **2006**, *250*, 3094–3117.
12. Black, C. B.; Andrioletti, B.; Try, A. C.; Ruiperez, C.; Sessler, J. L. *J. Am. Chem. Soc.* **1999**, *121*, 10438–10439.
13. Kleerekoper, M. *Endocrinol. Metab. Clin. North Am.* **1998**, *27*, 441–452.
14. Davis, F.; Collyer, S. D.; Higson, S. P. J. *Top. Curr. Chem.* **2005**, *255*, 97–124.
15. Chen, C.-L.; Chen, Y.-H.; Chen, C.-Y.; Sun, S.-S. *Org. Lett.* **2006**, *8*, 5053–5056.
16. Morozumi, M.; Hossain, R. Z.; Yamakawa, K.-i.; Hokama, S.; Nishijima, S.; Oshiro, Y.; Uchida, A.; Sugaya, K.; Ogawa, Y. *Urol. Res.* **2006**, *34*, 168–172.
17. Gunnlaugsson, T.; Davis, A. P.; O'Brien, J. E.; Glynn, M. *Org. Biomol. Chem.* **2005**, *3*, 48–56.
18. Gunnlaugsson, T.; Kruger, P. E.; Lee, T. C.; Parkesh, R.; Pfeffer, F. M.; Hussey, G. M. *Tetrahedron Lett.* **2003**, *44*, 6575–6578.
19. Bernard, V. *Molecular Fluorescence: Principles and Applications*; Wiley-VCH: Weinheim, Germany, 2001.
20. Wen, Z.-C.; Jiang, Y.-B. *Tetrahedron* **2004**, *60*, 11109–11115.
21. Atkinson, P.; Bretonniere, Y.; Parker, D. *Chem. Commun.* **2004**, 438–439.
22. Li, Z.; Chen, Y. H.; Jiang, Y. B. *Sci. China, Ser. B: Chem.* **2009**, *52*, 786–792.
23. de Silva, A. P.; Nimal, H. Q.; Gunaratne, N.; Gunnlaugsson, T.; McCoy, C. P.; Maxwell, P. R. S.; Rademacher, J. T.; Rice, T. E. *Pure Appl. Chem.* **1996**, *68*, 1443–1448.
24. Gunnlaugsson, T.; Ali, H. D. P.; Glynn, M.; Kruger, P. E.; Hussey, G. M.; Pfeffer, F. M.; dos Santos, C. M. G.; Tierney, J. *J. Fluoresc.* **2005**, *15*, 287–299.
25. Chung, S.-Y.; Nam, S.-W.; Lim, J.; Park, S.; Yoon, J. *Chem. Commun.* **2009**, 2866–2868.
26. Wei, L.-H.; He, Y.-B.; Wu, J.-L.; Wu, X.-J.; Meng, L.-Z.; Yang, X. *Supramol. Chem.* **2004**, *16*, 561–567.
27. Kato, R.; Nishizawa, S.; Hayashita, T.; Teramae, N. *Tetrahedron Lett.* **2001**, *42*, 5053–5056.
28. Anzenbacher, P., Jr.; Palacios, M. A.; Jursikova, K.; Marquez, M. *Org. Lett.* **2005**, *7*, 5027–5030.
29. Jose, D. A.; Kumar, D. K.; Ganguly, B.; Das, A. *Org. Lett.* **2004**, *6*, 3445–3448.
30. Ghosh, T.; Maiya, B. G.; Wong, M. W. *J. Phys. Chem. A* **2004**, *108*, 11249–11259.
31. Jradi, F. M.; Al-Sayah, M. H.; Kaafarani, B. R. *Tetrahedron Lett.* **2008**, *49*, 238–242.
32. Hu, J.; Zhang, D.; Harris, F. W. *J. Org. Chem.* **2005**, *70*, 707–708.
33. Elderfield, R. C.; Meyer, V. B. *J. Am. Chem. Soc.* **1954**, *76*, 1887–1891.
34. Cheeseman, G. W. H. *J. Chem. Soc.* **1962**, 1170–1176.
35. Kleineweischede, A.; Mattay, J. *Eur. J. Org. Chem.* **2006**, 947–957.
36. Bordwell, F. G. *Acc. Chem. Res.* **1988**, *21*, 456–463.
37. Fu, Y.; Liu, L.; Li, R.-Q.; Liu, R.; Guo, Q.-X. *J. Am. Chem. Soc.* **2004**, *126*, 814–822.